Design and Optimization of Navigation and Guidance Techniques for Mars Pinpoint Landing: Review and Prospect

Zhengshi Yu[1,2], Pingyuan Cui[*1,2], John L. Crassidis[3]

1. Key Laboratory of Autonomous Navigation and Control for Deep Space Exploration, Ministry of Industry and Information Technology, Beijing 10081, China

2. Institute of Deep Space Exploration, School of Aerospace Engineering, Beijing Institute of Technology, Beijing 100081, China

3. University at Buffalo, Buffalo, NY, 14260, USA

Abstract:

Future Mars landing missions will require the capability of precise landing at certain sites for specific scientific interests to gather more valuable scientific information. Autonomous navigation and guidance in the Mars approach, entry, descent, and landing (AEDL) phase plays an important role in fulfilling a pinpoint landing mission. This paper systematically summarizes the latest developments and current status of autonomous navigation and guidance designs for Mars landing missions. Firstly, the AEDL phase for Mars landing is analyzed, and several landmark Mars landing missions are reviewed. Based on the precision requirement, the technology challenges of autonomous navigation and guidance for Mars pinpoint landing are discussed. Then, recent developments of autonomous navigation design, which contain the navigation scheme and state estimation methods are summarized. Furthermore, the cutting-edge concept of navigation scheme optimization is also introduced, which may provide new ideas to the mission design. Next, the state-of-art guidance technologies of entry and powered descent phases are analyzed. The corresponding reachable and controllable set analysis, trajectory optimization, and advanced guidance methods are also revealed. Finally, aiming to support future Mars pinpoint landing missions, a comprehensive prospective for the development of autonomous navigation and guidance is presented.

1. Introduction

As the most similar planet to the Earth in the Solar system, Mars is considered as an ideal target for planetary exploration [1, 2]. Since the 1960s, humans have investigated the Mars exploration missions in the near distance. With the development of aerospace science and technology, the manner of Mars exploration has shifted from flyby/orbiting to landing and roving explorations. Considering scientific returns and exploration capabilities, Mars landing exploration is also essential and is one of the most popular tasks of human deep space exploration in the near future. The representative Mars landing missions including NASA's Viking 1 and 2, Mars Pathfinder (MPF), Mars Exploration Rovers (MER, including the Spirit and Opportunity rovers), Phoenix, Mars Science Laboratory (MSL, including the Curiosity rover), and ESA's Mars Express/Beagle 2 mission. All of these greatly inspire the development of advanced guidance, navigation, and control (GNC) technologies.

During the past 50 years of Mars exploration, 46 Mars exploration spacecrafts have been launched. The overall success rate is only 41.3% though. Furthermore, among the 20 Mars landing attempts, only 7 robotic rovers were successful. The success rate for Mars landing missions is only 35%. Among the failed landing missions, most failures occur during the landing phase. The statistics of Mars exploration missions are shown in Table 1.

It is indicated that the landing process is a critical and dangerous phase of the entire Mars landing mission. Meanwhile, future Mars landing missions may need the capability of landing at specific sites in order to guarantee the safety of the mission and to gather more scientific information. However, present

GNC technologies are mostly based on the Viking missions whose performance of the navigation and guidance system is no longer suitable for high accuracy and safety requirements. Therefore, new generations of GNC technologies need to be investigated to improve the accuracy and safety of successfully landing on Mars.

Table 1 Statistics of previous Mars missions

Mission Type	Success rate	Total missions	Successful missions	Failed during launch	Failed during cruise	Failed during landing
Flyby	37.5%	8	3	4	1	-
Orbiting	50%	18	9	5	4	-
Landing	35%	20	7	2	3	8
Total	41.3%	46	19	11	8	8

1.1 Mars Pinpoint Landing and AEDL Phase Analysis

The surface of Mars is covered by a thin layer of atmosphere. The density of the Martian atmosphere is 1% of that on the Earth, and the thickness of the Martian atmosphere is about 125 km [3]. The landing mission must experience the final approach, entry, descent, and landing (AEDL) successively. The final approach phase can be defined from about 12 hours before the entry point to the spacecraft reaching the upper layer of the atmosphere [4]. During this period, the spacecraft needs to process navigation to accurately estimate the conditions of the entry point and adjust the attitude and trajectory.

The entry phase begins when the entry vehicle reaches the atmosphere and ends when the parachute is deployed. At the beginning of the entry phase, the velocity of the entry vehicle can reach 4 to 7 km/s. Then the velocity may be decelerated to about Mach 2 by the aerodynamic drag. In this period, the vehicle estimates the position and velocity in real time, and the guidance and control system may control the entry vehicle to reach the parachute deployment condition by adjusting the sign and magnitude of the bank angle. The entry phase is the most dangerous and unpredictable period among the entire Mars landing process. During this phase, the entry vehicle may reach the peak deceleration and peak dynamic pressure. In order to protect the entry vehicle from large amount of aerodynamic heat caused by air friction, the entry vehicle is usually packed in the heat shield.

The descent phase can be further divided into parachute descent and powered descent phases. In the parachute descent phase, the velocity of the vehicle is further decelerated by the drag of the parachute. At the end of the parachute descent phase, the heat shield is discarded and multiple sensors can be initialized for the navigation in the following powered descent phase. The powered descent phase is determined from the start of the descent thruster to the stabilization of the descent stage. The purpose of this period is to eliminate the horizontal and vertical velocity, so that the system is ready for the final Mars landing. Comparing to the entry phase, a stronger maneuverability during the descent phase must be obtained. Therefore, possible obstacle detection/avoidance and guidance are conducted in this phase.

The landing phase is the final stage of the AEDL phase. In this phase, the rover needs to land safely on the ground, and the following scientific exploration mission can begin. The touchdown system of the rover can be divided into two main categories: the passive energy dissipation system and the active system. Besides the Mars Science Laboratory mission, the other six missions were landed by a passive energy dissipation system, such as an airbag or legs [3]. Although easy implementation and high reliability make the airbag a preferred choice for light weight rovers, the bouncing movements after landing greatly reduce the landing accuracy. Also, the legs are only suitable for the light weight rovers. Therefore, an active landing system such as the Sky Crane for the Curiosity rover is a possible solution for the future pinpoint landing of heavy rovers. The AEDL phase of the Mars Science Laboratory mission is shown in Fig. 1.

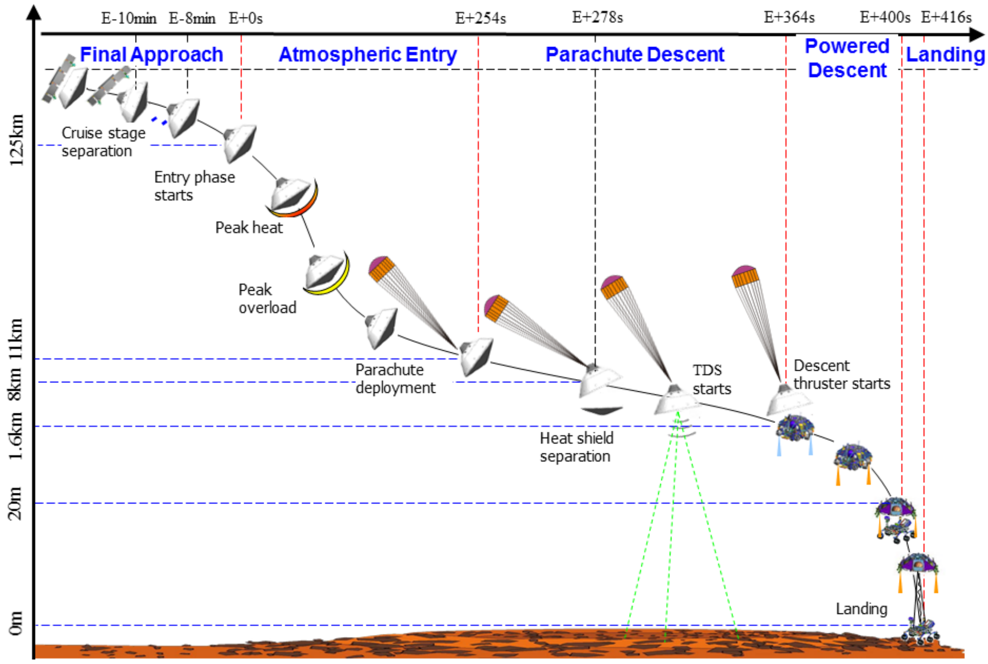

Fig. 1 The AEDL Phase of the MSL Mission [5]

1.2 Review of Landmark Mars Landing Missions

1.2.1 Mars Exploration Rover

The Mars Exploration Rover mission is part of the NASA Mars Exploration Program, a long-term effort of robotic exploration of the red planet. The twin Mars rovers, MER-A Spirit and MER-B Opportunity, landed on Mars on January 3 and January 24, 2004 separately. The primary scientific goal is to search for clues of past water activity on Mars.

During the cruise and approach phases, the navigation and orbit maneuvers were performed using the sensors and actuators mounted on the cruise stage. The development of the cruise stage is based on the Mars Pathfinder mission. The attitude determination was achieved using Sun sensors and star sensors, while the orbit determination was mainly based on radiometric measurements from NASA’s Deep Space Network (DSN) [6]. In the implementation, two-way coherent Doppler, two-way coherent ranging, and delta differenced one-way ranging (ΔDOR) were used as radiometric data. The entry descent and landing phases adopted the concept developed from the Viking and Mars Pathfinder missions. During atmospheric entry, the MER flew an unguided and ballistic entry trajectory. Litton LN-200 Inertial Measurement Units (IMU) mounted on the backshell in conjunction with the rover IMU were used to determine the position and velocity of the entry vehicle [7]. The parachute was then deployed according to the navigation results. In the descent and landing phases of the two rovers, a vision system called the Descent Image Motion Estimation System was employed. Such a system consisted of a descent imager and a radar altimeter, and could estimate the horizontal velocity during the last 2000 meters by tracking features on the ground from three images taken by the imager [8]. The estimation results were used to control the firing of the retrorocket in order to reduce the horizontal velocity before landing. For the final landing phase, airbags were used for the twin rovers to cushion surface impact. Meanwhile a radar altimeter mounted on the lower corner of the lander provided the distance measurements to the Mars surface, and determined to fire the Rocket Assisted Deceleration (RAD) system for final landing [9].

Both MER-A and MER-B achieved the predicted scientific and engineering goals. The performance of the developed navigation and control system was also demonstrated. The actual landing locations differed from the target landing points by 10.1 km for Spirit and 24.6 km for Opportunity. The majority of the landing position offsets for both landers were primarily caused by variations in atmosphere and spacecraft aerodynamic modeling from what was predicted. The amount of the landing position offset caused by navigation errors was only 3.3 km for Spirit and 9.7 km for Opportunity [10].

1.2.2 Mars Science Laboratory

The Mars Science Laboratory mission landed on the Mars surface in August 2012. The scientific goal was still to continue the search for evidence of life on Mars through numerous scientific instruments aboard a 900 kg rover. In order to achieve both the scientific and technology goals, the mission utilized advanced GNC technologies to significantly improve Mars pinpoint landing capability. Among the seven successful Mars landing missions, the MSL was the most expensive mission and represented the highest technology level in Mars landing explorations.

In the approach phase, the fundamental objective of navigation system for MSL is to ensure the spacecraft will arrive at the specified entry conditions at the correct time. Orbit determination was accomplished using DSN, Doppler, ranging, and ΔDOR measurements. Meanwhile, a star tracker and IMU were used for attitude determination [11]. After the vehicle entered the atmosphere, an inertial navigation system based on the IMU was activated to estimate the position and velocity of the entry vehicle. This navigation scheme was essentially based on the NASA's previous Mars landing missions. During the Mars entry phase, MSL utilized an offset center of mass to create an angle of attack, which is different from the spin stabilized entries of MER and MPF. More significantly, an entry guidance algorithm developed from the Apollo re-entry was used to guide the vehicle to arrive at the parachute deployment velocity close to the desired downrange, crossrange, and altitude [12]. To achieve a high landing altitude and high performance requirement, a single 21.5 m diameter supersonic parachute was designed. This is the largest parachute ever used for Mars landing missions. After the heatshield separation, a Terminal Descent System (TDS) could take direct measurements of altitude, attitude, and velocity relative to the surface using a 3-axis Doppler velocimeter and a slant range altimeter [13]. Before that, the vehicle's state was estimated by integrating IMU measurements. During the powered descent phase, a polynomial guidance law from the Eagle lander of the Apollo mission was used, and the descent stage followed a 3-D polynomial trajectory to reach 100 m above the surface with zero velocity [5]. Finally, a novel Sky Crane touchdown approach, which was the most innovative portion of the landing technologies, was employed [14]. The rover was tethered beneath the descent stage and was lowered onto the Martian surface directly. After landing, the connection with the descent stage was broken and the descent stage flew away from the rover.

The MSL extended the limits of the Mars landing technologies qualified by the Mars Viking, Mars Pathfinder, and Mars Exploration Rover missions. The Curiosity rover landed only 2.2 km east and 400 m north (less than 1σ errors) of the target [5]. The success of the mission has demonstrated several innovative GNC technologies and paved the way for future Mars landing missions.

1.3 Challenges for Navigation and Guidance Design for Mars Pinpoint Landing

The focus of the Mars exploration mission design is being shifted from mission safety to scientific goals. Future Mars missions may thus need the capability of precise landing at predefined locations of great scientific interest [1]. NASA has also emphasized the need for fundamental research on the navigation and guidance techniques for the pinpoint landing on Mars in the future [15], and proposed the future pinpoint landing accuracy of kilometers or even hundreds of meters. In order to fulfill the demand of pinpoint landing, high performance guidance and control have to be employed since the entry and powered descent phases, and an accurate navigation is indispensable during the entire AEDL phase.

However, the duration of the Mars landing is very short, but the time delay caused by the long distance is severe. Therefore, the traditional navigation and control methods based on the Deep Space Network are no longer appropriate for the Mars landing missions. Considering the complex and uncertain dynamic environment during a Mars landing, the limited navigation information, nonlinearity and uncertainty of the dynamic model, and the weak control capability are the main challenges which pose obstacles for the autonomous navigation and guidance with high performance.

1.3.1 Limited Navigation Information

The definition of limited navigation information can be divided into two main aspects. First, the limited navigation information means that the navigation measurement methods are restricted [2]. For example, in the Mars entry phase, the shelter of the heat shield results in the fact that multiple navigation sensors cannot function. Only the IMU can be used for inertial navigation. The second aspect is that the information of the vehicle’s states in the navigation measurements is not complete, which means that not all states of the vehicle can be accurately known [2]. Although a TDS which can provide the attitude, altitude, and velocity estimation was equipped on the descent stage of the MSL mission, the horizontal position of the vehicle couldn’t be estimated because no such information can be obtained by TDS measurements. Furthermore, even though a radiometric measurement based autonomous navigation has been proposed for Mars landing missions, the number of available beacons is still limited for a global coverage. These issues lead to weak observability and even full unobservability of the navigation system. Multiple constraints and requirements are put forward for the navigation system design.

1.3.2 Nonlinearity and Uncertainty of the Dynamic Model

After entering the Mars atmosphere, the entry vehicle flies at a hypersonic velocity. The aerodynamic force results in the high nonlinearities in the dynamic model. Meanwhile, uncertainties are presented in the atmospheric density and aerodynamic coefficients (e.g. lift and drag coefficients, ballistic coefficient, and lift-to-drag ratio). The most critical uncertainty lies in the atmospheric density [16,17]. Even though several Mars atmosphere models have been developed based on previous measurements and have been used in Mars mission designs, an accurate determination of atmosphere density can still not be achieved due to randomness and time-varying disturbances. Furthermore, the high speed of the spacecraft will cause the atmosphere ionization. This phenomenon may lead to an unexpected measurement noise, especially for radiometric measurements, which will also reduce the accuracy of the navigation filter. Therefore, how to achieve a high robustness under model parameter uncertainties and unmodeled measurement noise should be emphasized in the navigation filter design. These uncertainties and noise may limit the performance of both the navigation and guidance of the Mars pinpoint landing. How to develop the navigation and guidance algorithms to cope with the high nonlinearity and uncertainties should be especially considered.

1.3.3 Weak Control Capability

During the Mars entry phase, an offset center of mass is usually used to create an angle of attack. The bank angle, which can change the direction of lift force, is the only possible control signal to adjust the shape of the entry trajectory [18]. Compared with a winged flight vehicle, the lift-to-drag ratio is much smaller, and the control capability is weaker. Only a small range of maneuver can thus be achieved. Therefore, a reliable guidance system that can reach parachute deployment conditions while satisfying both downrange and crossrange constrains in an uncertain environment is very challenging [19]. Furthermore, for Mars powered descent and landing, the descent stage needs to reach the predefined landing site while avoiding potential obstacles and hazards. However, the horizontal moving ability as well as the carried fuel is limited. The uncertainties in the navigation and control system also influence the safety and reliability of the guidance system. So not only the fuel efficiency but also the navigation and control errors should be considered for guidance system design.

In order to solve such problems theoretically, the National Basic Research Program of China 2012CB720000 was proposed. As the first National Basic Research Program of China in the field of deep space exploration, this Program aims to provide new solutions to the GNC problem for planetary landing missions. The navigation and guidance for Mars pinpoint landing is the most significant research target. Funded by the Program, a thorough investigation of the navigation and guidance of the Mars landing was performed and abundant academic achievements were obtained. This paper reviews the research progress of the navigation and guidance for Mars pinpoint landing comprehensively, as well as demonstrated the results from the National Basic Research Program of China.

2. Review of Autonomous Navigation for Mars AEDL

An accurate navigation system is the foundation of the guidance and control for Mars pinpoint landing. In this section, the research developments of the autonomous navigation for Mars landing will be reviewed. The main problems encountered will also be summarized.

2.1 Navigation Scheme

A navigation scheme with reliability and high performance is the foundation of an accurate state estimation. Therefore, the question of how to design the navigation scheme in the presence of limited navigation information should be answered at first. This section summarizes the development of the navigation scheme for a Mars landing which may inspire the requirements for an accurate navigation system design.

2.1.1 Navigation Scheme for the Approach Phase

The knowledge of the entry condition, especially flight path angle (FPA), may have significant impact on the accuracy of the aerocapture and pinpoint landing. Therefore, real-time navigation during the final approach phase of a Mars landing mission is an important contributor to fulfilling the requirement of future Mars exploration.

The radio antennas of NASA's Deep Space Network, which are located in Goldstone California, Madrid Spain, and Canberra Australia, together with the radio system mounted on the spacecraft, are primarily utilized to provide navigation measurements for Mars exploration missions [20]. The traditional measurements of radiometric Doppler and range are used by Mars exploration missions in most mission phases to determine the spacecraft radial velocity and range. Furthermore, in order to improve the navigation performance by determining the spacecraft angular position, ΔDOR measurements are employed in conjunction with Doppler and range data [21]. The Mars Science Laboratory mission used these three types of tracking information from the DSN as assessments of the spacecraft's trajectory [11]. Navigation during the cruise and initial approach phase mostly relies on ground-based Earth observations because there is sufficient time to relay telemetry and uplink commands to the spacecraft. However, the final approach phases are short and the navigation must be performed without ground-based Earth support because of severe time delays. So the trajectory knowledge updates after the ground based data cutoff, which is typically 6h before entry, should be obtained in situ and processed onboard.

Optical measurements have been used for autonomous navigation in Mars exploration missions. The optic center of the planetary target or its natural satellites could be extracted after image-processing, and the direction vector from the spacecraft to the center of the target or the angles between the target center and background stars could be used to determine the spacecraft's orbit [22-25]. However, with the rapid decreasing distance to Mars, the image of the planet will gradually occupy the entire field of view, which may lead to difficulties in extracting the optic center of Mars. Therefore, the optical navigation cannot provide a complete navigation service in the final approach phase.

The Mars Network which is composed of Mars orbiters could be ideally located to provide spacecraft-to-spacecraft radiometric navigation data, which is useful for a navigation scheme design [26,27]. Using the Electra ultrahigh frequency (UHF) transceiver, relative radial velocity and range can be provided by processing the data of Doppler and range measurements. Therefore, the navigation can be processed onboard in real time during the final approach. Ely examined the performance of the Mars Network of providing approach navigation services given certain tracking capabilities, and showed that the Mars Network Doppler was a robust data type which could improve the trajectory knowledge accuracy [28]. Lightsey conducted a set of analyses based on the MSL mission combined with the Mars Reconnaissance Orbiter (MRO), and demonstrated that the navigation system could achieve a 300m entry knowledge error [29]. However, because of the occlusion of Mars, the line of sight visibility between the spacecraft and the orbiter does not exist all the time. A real-time and autonomous navigation during the whole approach phase cannot be achieved.

In recent years, X-ray pulsars have been considered as potential sources for deep space navigation[30,31]. X-ray pulsars, which are highly magnetized and rotating neutron stars providing stable, predictable, and unique signatures, give a new answer to autonomous navigation for Mars final approach. The navigation system utilizing X-ray pulsars is available where X-ray pulsars can be observed. Furthermore, the system can operate in an autonomous mode, independent of the DSN systems. In previous investigations, the possibility and algorithms of autonomous navigation using X-ray pulsars have been widely investigated [32-35]. NASA has started the XNAV program to demonstrate the feasibility of X-ray pulsars based navigation and has developed related payload and software [36]. More recently, in 2011, NASA Goddard Space Flight Center started the Neutron-star Interior Composition Explorer (NICER) mission [37]. The involving project of the Station Explorer for X-ray Timing and Navigation Technology (SEXTANT) investigated X-ray pulsar-based autonomous navigation for deep space exploration [38]. Based on the benefits of autonomy and accuracy, navigation using X-ray pulsars may be a supplementary means of real-time navigation for Mars final approach. Cui et al. introduced X-ray pulsar measurements to design the navigation scheme for Mars final approach (see Fig. 2) [39]. According to this navigation scheme, the Fisher information matrix was used to optimize the navigation pulsars from the pulsar candidates to further improve the navigation performance. The 3σ uncertainties of position, velocity, and flight path angle at entry point can reach 1000m, 1m/s, and 0.02deg, respectively. However, at the end of the final approach phase, the nonlinearity of the dynamic system increases rapidly. The navigation system depending solely on the X-ray pulsars will thus lead to degradation and even divergence, particularly for velocity and flight path angle. To cope with this problem, Cui et al. combined the X-ray pulsars with the Mars Network in the later period of the Mars final approach. An improved estimation performance can thus be achieved because of improved observability [40].

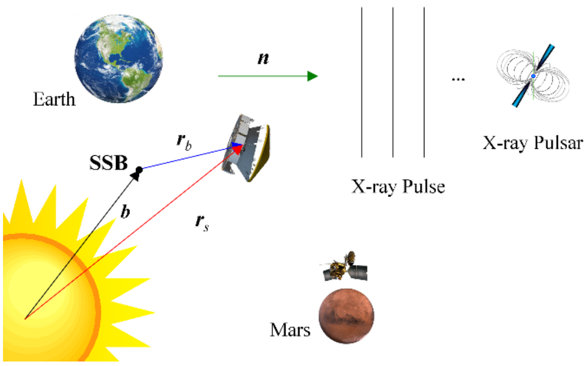

Fig. 2 X-ray Pulsar-Based Navigation Scheme for Mars Final Approach Phase [39]

2.1.2 Navigation Scheme for the Entry Phase

As NASA's first successful soft landing missions, Viking 1 and 2 provided technology support for follow-up Mars landing missions, especially for the AEDL phase. The inertial navigation scheme has been inherited and developed from the Viking missions. The inertial navigation based on the IMUs is the most developed and the only possible method during the Mars entry phase at present. Up to now, the IMU LN-200 developed by Litton Corporation has been used on the Spirit, Opportunity, and Curiosity vehicles. The newest ESA Mars lander, named Schiaparelli also used the same inertial navigation scheme. However, the overflow of IMU output for just one second leaded to the misinterpretation of altitude and ignited the ensuring landing process at a wrong time, which finally resulted in the crash of lander [41]. The failure of Schiaparelli indicates that this sole inertial navigation scheme is not reliable during atmospheric entry. Furthermore, the accuracy of the inertial navigation depends on the estimation accuracy of the initial entry condition. The drift/bias together with measurement noise all influence the navigation performance. Therefore, additional potential navigation information should be combined with the inertial navigation to further correct the initial estimation error.

In order to perform autonomous navigation without other sensors, IMU-based navigation schemes have been proposed. Ely et al. first introduced an explicit model of the atmosphere density, and built the measurement model of the accelerometer as a function of the altitude and velocity of the vehicle [42]. Therefore, the accelerometer output could be treated as measurements and the state of vehicle can be estimated by extended Kalman filter (EKF). The feasibility of this navigation scheme was also investigated. However, because of the introduction of the atmosphere density model, the accelerometer-based navigation scheme is sensitive to model errors of the atmosphere density. In order to alleviate he sensitivity of the navigation accuracy, Heyne proposed a model-based navigation algorithm using an unscented Kalman filter (UKF) [43]. Based on the same navigation scheme, Dubois-Matra and Zanetti proposed a multi-model-based adaptive filter, and demonstrated the improved robustness of the navigation algorithm to the uncertainty of the atmosphere density model [44,45]. Although the IMU-based navigation scheme could improve the navigation performance, the amount of navigation information is still limited. An accurate prior knowledge of the atmosphere density should also be given.

Meanwhile, Kenneth proposed an autonomous formation flying sensor concept for precise relative position and attitude determination for the spacecraft where real-time or near-real-time knowledge of relative position and attitude was required [46]. This concept provided a new direction for the entry navigation scheme design. It has been reported that high frequency radio signals could penetrate the plasma sheath during Mars entry [47]. According to this research, a Mars Network-based entry navigation scheme was proposed, which is shown in Fig. 3 [48]. In the implementation, radio measurements between the spacecraft and radio beacons such as Mars orbiters or ground based beacons (whose position and velocity could be determined in advance) are proceeded via high frequency transceivers. The amount of navigation information is thus increased greatly. Lightsey et al. researched NASA's embedded navigation scheme using radiometric data from UHF spacecraft-to-spacecraft links which was processed to determine position and velocity in real time [29]. Burkhart et al. also investigated a similar navigation scheme, and demonstrated that an improved state knowledge and the performance of entry guidance could be provided [49]. Lévesque combined the IMU with the radiometric measurements, and proposed an algorithm to estimate the vehicle's position, velocity, aerodynamic coefficient, and atmosphere density [50]. The observability of the navigation system was also discussed. Hastrup et al. further developed a low cost Mars Network concept, and proposed a two-layer network for accurate navigation for a Mars landing [27]. Yu et al. investigated the possibility of using radiometric measurements in the Mars entry, descent, and landing phases, and showed the improved navigation performance over the MSL landing scenario [51].

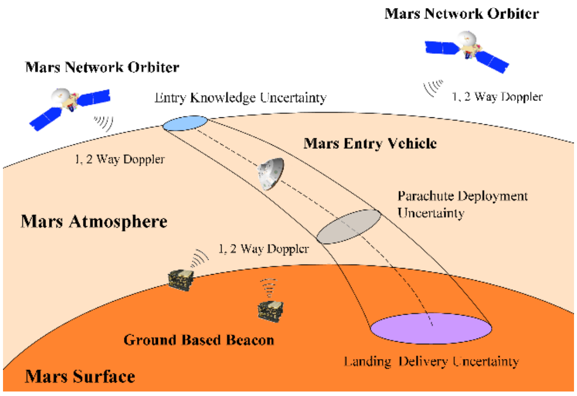

Fig. 3 Mars Network-Based Navigation Scheme for Mars Entry [48]

The UHF transceiver Electra, developed by NASA's Jet Propulsion Laboratory is the major telecommunication payload for Mars exploration missions [52], and has been equipped in the MRO and MSL missions. It is desired to provide accurate trajectory determination for future Mars missions. During the entry phase of the MSL, the capability and reliability of UHF relay communication have been demonstrated [53]. Although only Doppler signals can be provided, NASA is still updating the configuration and algorithms. The programmable configuration could make Electra flexible and reliable for the navigation system of Mars landing missions [54].

On the other hand, although many navigation sensors are wrapped in the heatshield, the pressure can still be measured using certain sensors placed on the heatshield. Actually, similar measurements have been obtained in previous Mars landing missions [55]. In both Viking entry vehicles, pressure and temperature sensors were mounted and provided the first atmospheric data of Mars. In the MSL mission, a completely new sensor called the Mars Entry Atmospheric Data System (MEADS) was used to record the pressure distribution around the fore-body of vehicle during the entry phase. The MEADS has demonstrated the capability of accurate determination of the dynamic pressure and atmospheric density during Mars entry. The MEADS made use of 7 flush pressure measurements on the heatshield fore-body to allow estimation of atmospheric parameters. In particular, the accuracy objective of dynamic pressure is within 2% in the 3σ sense [56]. At present, these measured pressures, together with triaxle accelerometer, are used to obtain the estimation of atmospheric quantities and to reconstruct the vehicle's entry trajectory [57, 58]. On the other hand, considering the concept of the IMU-based navigation scheme, if the atmospheric density model is also introduced, then a measurement model of the dynamic pressure can be developed, which can be used to estimate the state of the vehicle with certain filters. This concept also makes the dynamic pressure-based navigation a potential navigation scheme for Mars entry.

2.1.3 Navigation Scheme for the Powered Descent Phase

After the heatshield separation, the state of the vehicle may deviate from the nominal value due to disturbances during the parachute descent phase. Meanwhile, complex and uncertain terrain conditions on the Mars surface call for accurate guidance and control for the final pinpoint landing [59]. Therefore, reliable and accurate navigation which can determine the position, velocity, and attitude simultaneously becomes particularly important.

The navigation for the powered descent phase can be divided into two main categories: relative navigation and absolute navigation. Absolute navigation involves determining the coordinates of the lander with respect to the absolute frame such as the Mars landing frame or the Mars inertial frame. Unlike absolute navigation, relative navigation works out the coordinates of lander in a relative coordinate frame based on the relative measurements. For velocity and attitude, absolute navigation can almost be achieved. However, due to the lack of an absolute position reference, the estimation of position is usually based on the relative navigation.

Light Detection and Ranging (LIDAR) can provide both position and velocity estimation, and the ability of hazard avoidance under any illumination condition based on the terrain relative navigation (TRN) [60-62]. However, a reference digital elevation map (DEM) of the landing site with high definition should be provided in advance. Furthermore, the terrain feature matching is a complicated and time consuming work. An alternative instrument involving Doppler LIDAR is capable of providing precise velocity measurements relative to the sensor reference frame, vehicle platform altitude, and attitude. Direct or indirect measurements of the lander's states can be integrated with the IMU output to obtain low-cost and robust estimation without the help of terrain information [63-65]. A similar navigation scheme can also be constructed in conjunction with the altimeter and velocimeter [66,67]. In the latest MSL mission, a navigation scheme based on the Terminal Descent System was used to determine the velocity, altitude, and attitude of the landing vehicle by radiometric measurements of six independent radar beams [13]. However, this navigation scheme cannot determine the absolute horizontal position. Therefore, the initial position error in the powered descent phase still cannot be mitigated.

Meanwhile, the vision aided navigation, which integrates the inertial measurement system and the navigation camera as well as the computer vision algorithms, is another kind of navigation scheme during the Mars powered descent phase, and has been considered for planetary landing [68-71]. For the Mars Exploration Rover mission, a Descent Image Motion Estimation System was mounted to estimate the horizontal velocity by comparing the rotation and translation between three sequent images [8]. In the algorithm, no absolute positions of features are needed, so the speed of computation is acceptable. At the beginning of the powered descent phase, a relatively high altitude guarantees a wide field of view. In this period, multiple features of the Mars surface (e.g. craters) can be used for navigation [72]. With the decreasing of altitude, the field of view grows narrower, and only point features in the images can be obtained.

Considering the limitations of above relative and absolute navigation methods, relative and absolute optical navigation methods can be combined together to improve the navigation performance. On the other hand, artificial beacons can be alternatively considered as absolute position references. Therefore, complex feature matching in absolute optical navigation is no longer needed. Yu et al investigated the possibility of introducing radiometric measurements in the Mars powered descent phase [73]. Furthermore, a real-time integrated navigation scheme was proposed using radiometric measurements from the ground beacons, navigation camera, Doppler radar, and IMU, and demonstrated the achievable navigation accuracy (see Fig. 4). Qin et al. proposed an integrated navigation scheme combining radiometric measurements from a Mars orbiter [74]. The improved absolute navigation accuracy and low computation cost also indicated the potential implementation for a Mars landing.

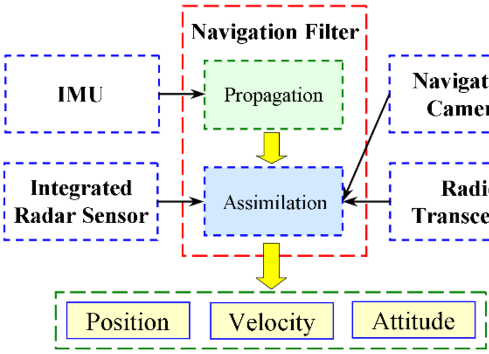

Fig. 4 Diagram of the Integrated Navigation System for the Powered Descent Phase [73]

2.2 State Estimation Method

The navigation filter plays an important role in fulfilling an accurate and stable state estimation for autonomous navigation. The most widely used approach is the EKF. However, the errors caused by the first-order Taylor series approximation may influence the convergence and accuracy, especially with a highly nonlinear dynamic model used for the Mars entry. The estimation errors may be reduced if the state propagation and assimilation can be performed directly through the nonlinear system. Monte Carlo based Kalman type filters have been of interest in recent years. For example, the ensemble Kalman filter (EnKF) has been adapted in many applications. In this algorithm, a set of ensemble elements are generated using Monte Carlo sampling for the uncertain states. These elements are then propagated through the nonlinear dynamic model and are used to calculate the optimal by Kalman gain [75]. The EnKF is more practical for high-dimension systems for which the covariance matrix may cause issues. Several variations of the EnKF, for example the ensemble square-root filter (EnSRF), have been developed to gain efficiency [76,77]. Particle filters are also ensemble-based assimilation methods dealing with nonlinear dynamic systems and non-Gaussian uncertainties, and have been applied in GPS/INS navigation and target tracking [78,79]. But they are not practical for high-dimension systems because of inefficient sampling. Similar approaches include the UKF, in which the Unscented Transformation (UT) is introduced, and a series of sigma points are employed instead of Monte Carlo sampling to capture the mean and error covariance [80,81]. However, the UKF is only suitable for Gaussian distributions, and UT is not always the optimal sampling approach [82]. To cope with these problems, Fu et al. introduced the optimal rank sampling principle and proposed the rank filter (RF) [83]. The RF is suitable for any distribution and achieves a more accurate propagation of state uncertainties. The relatively low computation cost gives the RF possibilities for practical applications.

The polynomial chaos (PC), which has been successfully evolved into the entire Askey scheme of orthogonal polynomials, has been proven to be more computationally efficient than Monte Carlo methods for propagating uncertainties in stochastic systems [84], and has already been used for state and parameter estimation. Pence et al. combined polynomial chaos theory with maximum likelihood estimation, and proposed a gradient based parameter update law [85]. Li and Xiu introduced the polynomial chaos expansion to the EnKF formulation [86]. The coefficients of polynomial chaos could be updated with high accuracy. Pajonk proposed a polynomial chaos-based non-Gaussian Bayesian estimator for state estimations of dynamical models, which did not require assumptions about the Gaussian distribution of the states [87]. Pajonk also developed a square-root approach to update the coefficients of polynomial chaos [88]. Blanchard presented a polynomial chaos-based Kalman filter for parameter estimation of mechanical systems, in which the error covariance matrix was computed by polynomial chaos expansion, and the Kalman based update was utilized to estimate the polynomial chaos representation of uncertain states [89]. More recently, Yu et al. introduced polynomial chaos theory to the state estimation problem based on a square-root implementation, and proposed the polynomial chaos-based square-root Kalman filter for Mars entry navigation, which extended the scope of polynomial chaos-based filters for Mars landing navigation [90].

For the Mars entry integrated navigation, the dynamic model is closely related to the Mars atmospheric density and the aerodynamic coefficients of the entry vehicle, which cannot be determined accurately. In order to reduce the impact of parameter uncertainties on degradation of state estimation, research has mainly focused on two directions: parameter approximations and parameter sensitivity reduction. Ely et al. used a Hierarchical Mixture-of-Experts (HME) filter bank as the estimation method, in which the filters are parameterized with various atmospheric density models and vehicle aerodynamic coefficients, and the HME filter bank selects the best model closest to the actual deviation [42]. Similar approaches include the Multiple Model Adaptive Estimation (MMAE) structure and its modification, in which the MMAE is used for Mars entry navigation in order to deal with the uncertainty of the atmospheric density [91,92]. Other scholars carried out research from the point of parameter sensitivity reduction, which describes the direct effect of the uncertain parameters on state estimation. The desensitized EKF, evolved from desensitized optimal control, is obtained by minimizing a cost function consisting of the posterior covariance matrix trace penalized by a weighted norm of the state estimate error sensitivities, exhibiting reduced sensitivity to deviations in the assumed dynamic model parameters for Mars entry integrated navigation[93-95].

2.3 Optimization of Navigation Information

Although the Mars Network-based navigation scheme has been proposed for the Mars AEDL phase, the configuration of the Mars Network is a main contributor to the navigation performance. In order to achieve an accurate navigation performance, the configuration of the Mars Network has to be optimized. This is also a novel concept to the navigation system design. Among previous research, Ely first presented and discussed the navigation requirements, drivers, and metrics to arrive at a preliminary constellation design [96]. Further, constellations around Mars for navigation were optimized using the performance index of Mean of the Position Accuracy Response Time (MPART) [97]. Pirondini designed Martian navigation constellations envisioned in the ESA’s Martian Constellation for Precise Object Location program focusing on the number of orbiters and the visibility [98]. These previous activities mostly extended the optimization methods of Global Positioning System (GPS) network to the Mars network and mainly focused on the global navigation performance. But the quantity of the Mars orbiters or ground-based beacons, which can provide radiometric measurement, is too limited to provide the tracking coverage of the vehicle during the entire AEDL phase. Currently the Mars network contains three NASA orbiters (Mars Odyssey, Mars Reconnaissance Orbiter, and Mars Atmosphere and Volatile Evolution). Therefore, a local performance for a specific mission instead of the global performance such as global coverage should be proposed to optimize the network configuration.

Pastor discussed the impact of beacon locations on the navigation performance during Mars entry phase, and chose the best configuration of the ground-based beacons among different possible beacon positions by analyzing the navigation accuracy from the EKF with radio measurements [99]. More significantly, Yu et al. analyzed the observability of Mars entry navigation which was an index associating the navigation accuracy. Meanwhile, the line-of-sight visibility was considered as a constraint and the beacon configuration was optimized using genetic algorithms [48,100]. Furthermore, Yu used the Fisher information matrix to investigate the relationship between the network configuration and the navigation accuracy [101]. Considering the range measurements from N ($N \geq 3$) beacons, the determinant of Fisher information matrix, which can be used to quantify the degree of observability, was derived by

$$\det(\boldsymbol{F}_N) \leq \sigma_{R\min}^{-6} \sum_{1 \leq k_3 < k_2 < k_1 \leq N} \left[\boldsymbol{n}_{k_1} \cdot (\boldsymbol{n}_{k_2} \times \boldsymbol{n}_{k_3}) \right]^2 \tag{1}$$

where $\sigma_{R\min}$ is the minimal standard deviation of measurement noise, and $\boldsymbol{n}$ denotes the unit position vector from the beacon to the entry vehicle. This equation establishes the relationship between the configuration of beacons with the navigation performance, and the resulting conclusions are useful for the navigation system design. Furthermore, focusing on the navigation scheme using only one or two beacons, Zhao et al. proposed a Fisher information-based optimization method [102].

3. Review of the Guidance for Mars Landing

3.1 Flight Performance Analysis

Before the design of entry guidance, the flight performance of the vehicle during the entry, descent and landing phase has to be analyzed to determine the nominal landing scenario. For Mars entry and landing, reachable and controllable set analyses are beneficial methods to design the trajectory envelope and nominal entry point and landing site, both of which are means of characterizing the trajectory performance of a vehicle.

The analysis of reachable set and controllable set has been introduced into the Mars atmospheric entry [103] and powered descent phase [104], where the reachable set denotes the set of the terminal states that can be reached from the nominal initial state, while the controllable set is the set of initial states from which the nominal terminal target can be achieved (which emphasizes on the initial flight path angle for Mars atmospheric entry and is related to the concept of entry corridor [103]). More systematically, Eren et al. analyzed the reachable and controllable set in the presence of all relevant control and mission constraints for Mars powered descent phase with a convex optimization method which is of benefit for the off-line design and analysis for a powered descent vehicle as well as the onboard capability of decision making in future missions [104].

To deal with the severe impact of model uncertainties on planetary landing safety and accuracy, controllable union set (CUS) analysis and controllable intersection set (CIS) analysis were conducted (see Fig. 5), respectively, to improve the robustness of entry state selection and entry trajectory to model uncertainties [105]. The CUS and CIS for Mars entry phase were analyzed specifically by considering the uncertainties in ballistic coefficient, lift-to-drag ratio, and the atmospheric density. Meanwhile, the contribution of uncertainties to the size of the CUS and CIS was also discussed. The conclusions not only were useful for the selection of the entry point, but also could help improve the robustness of entry trajectory.

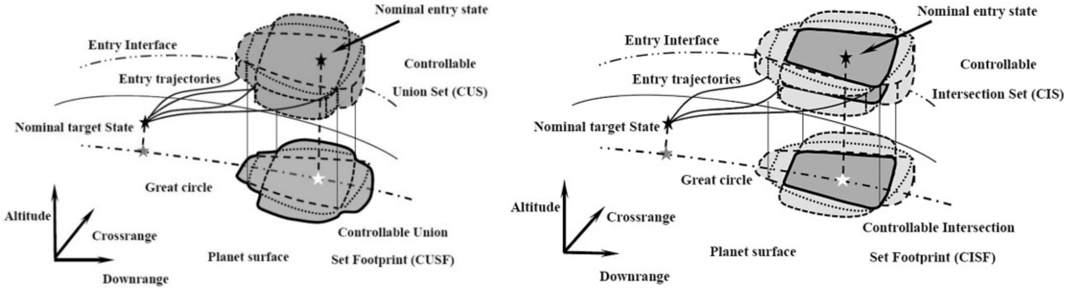

Fig. 5 Concept of Controllable Union Set and Controllable Intersection Set [105]

3.2 Reference Trajectory Generation

Reference trajectory optimization is an important prerequisite for the implementation of guidance and control. A well-designed entry trajectory can preplan the landing scenario while meeting multiple constraints, which increases the safety of missions. Considering the computation complexity and the potential real-time application, the reference trajectory generation can be divided into two main categories: off-line trajectory optimization and on-line trajectory generation.

3.2.1 Off-Line Trajectory Optimization

The off-line trajectory is usually adopted as the reference trajectory and calculated before the mission. Therefore, the computation cost is not the main consideration. Instead, efforts are put on how to find the optimal trajectory under multiple complex constraints.

The essence of off-line trajectory optimization is to solve an optimal control problem with complex constraints. The solving methods can be traditionally divided into two categories: indirect and direct approaches. In the indirect approach, the optimal control problem is solved by the maximum principle. However, the sensitiveness to the initial guess of the conjugate variables, which have no physical meaning, together with the low efficiency of a shooting method or multiple-step shooting makes indirect approaches difficult to be directly applied to the trajectory optimization for Mars atmospheric entry [18,106]. Therefore, the majority of previous research using indirect approaches were based on very simple dynamics and constraints [107,108].

On the other hand, as one of the most important direct approaches, pseudospectral methods are typically used to transfer the trajectory optimization problem to a static nonlinear programming problem. Various pseudospectral methods have been proposed for trajectory optimization problems [109,110]. The high accuracy and fast convergence make pseudospectral methods an ideal solution for Mars atmospheric entry trajectory optimization [106,111-113]. Meanwhile, several integrated software packages like GPOPS have been developed to free engineers from complicated programming and computing [114]. However, their applications are still restricted because of the significantly high computational cost. Also, global optimality cannot be guaranteed.

In recent years, the fast development of intelligent global searching methods provided a new direct method to solve the trajectory optimization problem. On one hand, it can be used for the initial guess of the costates in an indirect method [115]. On the other, it can be applied to solve the optimization problem directly. Lavagna presented the possibility of using particle swarm optimization techniques to define the optimal guidance history and the configuration of each different flight regime for an atmospheric entry vehicle [116]. Grant developed the single objective particle swarm optimization algorithm and multi-objective particle swarm optimization algorithm to improve the time-consuming traditional optimization methods [117]. Arora and Chen optimized the entry trajectory for a reusable entry vehicle using genetic algorithms considering dynamic pressure and heat flux constraints [118,119]. Yokoyama combined the genetic algorithm with a gradient-based optimization method and solved the trajectory optimization problem for planetary entry [120]. Lafleur searched the optimal Mars entry trajectory with the maximum-terminal altitude using a particle swarm optimizer [121]. In the algorithm, the entry flight path angle along with ten bank angle profile points were considered as optimization variables. Yu et al. discretized the entry flight path angle considering the value of dynamic pressure to improve the accuracy [122]. Meanwhile, for the fixed parachute deployment conditions, a backward integration was used and the observability-optimal trajectory was calculated based on the genetic algorithm.

Another typical direct method that has been rapidly developing in the recent years is convex optimization. It was first proposed to deal with the nonconvex control constraints and formulated the trajectory optimization problem as a finite dimensional semidefinite program which could be effectively solved using interior point algorithms [123]. Up to now, convex optimization still represents the state-of-the-art off-line trajectory optimization by considering both convex and non-convex constraints and ensuring global optimality of fuel consumption performance. At first, the computation of optimal trajectories was not likely to be conducted on-line due to the limitations of flight computers. Recently, after years of modification, a customized interior point method for onboard powered-descent guidance was presented [124], making it possible for on-line application.

Although various approaches have been used in the trajectory optimization of Mars atmospheric entry and landing, most of the previous research mainly focuses on the safety of mission. The altitude and velocity at parachute deployment are mainly considered. However, the initial entry state and the atmosphere density are the main disturbances during the Mars entry. The uncertainty in the state trajectory may cause the violation of path and boundary constraints. Therefore, in order to further develop the trajectory optimization technology for Mars landing, the disturbance of dynamic model as well as the observability of the navigation system have to be emphasized. Lafleur discussed the treatment of robustness as a distinct objective, and optimized the entry trajectory considering the altitude performance and error-ellipse robustness [125]. Li et al. introduced desensitized optimal control to reduce the sensitivity of the dispersion of the optimal trajectory [126]. Also, Yu et al. gave a potential solution to the robust trajectory optimization [127]. By introducing the polynomial chaos to describe the uncertainty propagation, the standard deviation and mean value of both states and constraints were determined. A modified robust trajectory optimization problem (see Fig. 6) can be built and solved by pseudospectral methods.

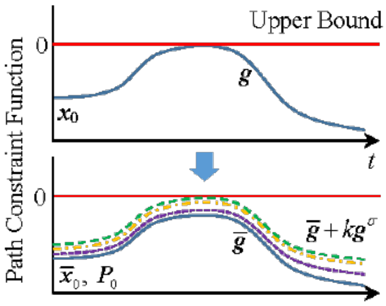

Fig. 6 Modification of the Robust Trajectory Optimization Problem [127]

3.2.2 On-Line Trajectory Generation

Considering the low control authority of the Mars entry vehicle and the large uncertainties existing in the entry environment, the capability of generating and updating feasible trajectories on-line has been pursued by researchers and mission designers. Feasibility means that the initial and final state conditions, the path and control constraints, as well as the nominal equations of motion are all satisfied. Tu et al. used polynomials to approximate the reference drag acceleration and modulated the coefficients to meet the range requirement [128]. Leavitt et al. have developed an approach to construct a more easily tracked drag profile by pre-tracking and interpolation [129]. Pre-tracking makes the upper and lower bounds of the drag-energy feasible to fly, while helps the entry vehicle to keep the ability to reach a wider footprint. However, interpolation of pre-tracked drag profiles may still be difficult for Mars entry vehicles to track, due to its weak control authority.

Accounting for landing safety and accuracy, high-altitude parachute deployment becomes the focus of the Mars entry trajectory design. Taking the deployment altitude and control authority of the deployment altitude as the performance index, Benito attempted to find the characteristics of the optimal entry trajectories, and developed an on-line trajectory generation method by planning the bank angle profiles, with three parameters corresponding to downrange, crossrange and deployment altitude respectively [130,131]. Considering the fact that searching for three parameters on-line was still time consuming, Duan et al. reduced the parameter number from three to one by slightly refining the trajectory updating model developed by Benito [132].

Meanwhile, considering the perturbations in the entry phase, sensitivity theory has been introduced to investigate the entry dynamics and design the on-line trajectory generation algorithm. Seebinder et al. developed a computationally feasible method to generate near-optimal trajectory trajectories from off-line optimized trajectories based on a parametric sensitivity analysis of nonlinear programs [133]. Zheng et al. innovatively developed two analytical reference drag profile update algorithms, i.e., the constant update algorithm and the linear update algorithm, for the drag-based Mars entry guidance based on parameter sensitivity theory [134]. The proposed method has the advantage of being iterative-free, which makes the algorithm computationally fast for on-line use.

Due to the uncertainties existing in the initial conditions, aerodynamic parameters and atmospheric densities, as well as the low control authority of the Mars entry vehicle, on-line trajectory generation and trajectory tracking guidance is promising for future Mars atmospheric entry guidance. The trajectory re-generation process may help the entry vehicles to reduce the tracking errors effectively. However, as the entry process is quite short, the trajectory generation algorithms should be computationally acceptable and reliable.

3.3 Trajectory Tracking Guidance Methods

The development of path-tracking guidance for Mars entry can be divided into two generations [135]. The first generation is based on the re-entry guidance of the Apollo capsule. In the algorithm, the downrange error is estimated using a linearized dynamic system about the nominal trajectory [136]. Although the nominal trajectory is not used for tracking, the generation of the guidance command relies on the nominal trajectory. Meanwhile, if the algorithm is modified to null the downrange error at different segments on the nominal trajectory, then this algorithm can also be treated as a path-tracking guidance. Carman and Mendeck investigated the use of a reference-path guidance method derived from the Apollo guidance system for a precise Mars landing [137,138]. Actually, the Apollo-based technique is the current baseline guidance scheme for the MSL mission [12].

The second generation is developed for the spacecraft with relatively large lift-by-drag ratios, such as space shuttles. In the algorithm, the nominal trajectory is defined as a drag acceleration-to-velocity or drag acceleration-to-energy profile. The bank angle command is generated to null the variation between the actual and nominal drag acceleration [139]. Theoretically, the design of the guidance algorithm can be expressed in an equivalent feedback control law approach, which is of great interest in previous researches. Bharadwaj introduced feedback linearization theory to the re-entry guidance of the space shuttle [140]. Then Saraf extended the algorithm to the 3-dimensional trajectory and proposed the Evolved Acceleration Guidance Logic for Entry (EAGLE) algorithm [141]. Tu modified the space shuttle guidance and proposed a drag-based predictive tracking guidance for the entry scenario taken from the NASA Mars Surveyor 2001 mission [128]. Lu employed receding horizon control and developed a closed-loop path-tracking guidance law based on a linear time-varying model [142]. Cho introduced differential geometry theory to the path-tracking guidance, and developed the guidance law based on a pursuit guidance method. The stability of the guidance law was also analyzed to follow constant-curvature paths [143].

The previous researches on the guidance for the Earth re-entry and Mars atmospheric entry have provided adequate references for the development of future Mars entry guidance. However, the navigation of Mars entry is still not accurate enough, which leads to relatively large errors in the entry vehicle's states. Furthermore, the atmospheric density cannot be determined accurately. These uncertainties are the major contributors to the tracking error which may cause the violation of path constraints and even the invalidation of the guidance law. In order to improve the path tracking performance under multiple uncertainties, Furfaro et al. proposed a nonlinear guidance scheme called Multiple Sliding Surface Guidance (MSSG) to follow the reference trajectory [144]. Based on higher order sliding control mode theory, a globally stable guidance command under bounded disturbances could be generated. Dai et al. adapted the Terminal Sliding Mode Control (TSMC) to account for the specific sliding mode exhibited by the longitudinal dynamics of the entry vehicle [145]. Dai also introduced the extended state observer (ESO) in the entry guidance design. More recently, a robust path-tracking guidance method based on model prediction control was proposed by Yu et al. The uncertainty of the atmospheric density was considered, and the propagation of tracking error was calculated to derive the guidance law [146].To alleviate the impact of undesired uncertainties, Li et al. developed a second-order sliding mode control based on a radial basis function neural network (RBF-NN) [147]. Talole used the perturbation observer to estimate the drag, drag rate, and the modeling error. The additional tracking error caused by model deviation can thus be reduced [148]. Xia introduced the active disturbance rejection control (ADRC) to the path-tracking guidance preliminarily. The feasibility and the robustness of the proposed guidance law were also demonstrated [149].

3.4 Trajectory-Independent Guidance Methods

A reference trajectory is indispensable for the trajectory tracking guidance no matter if the trajectory is generated off-line or on-line. In this section, another kind of guidance method, which is called trajectory-independent guidance is reviewed. Unlike trajectory tracking guidance, a preplanned trajectory is no longer needed. The numerical predictor-corrector guidance is a representative method.

The basic concept of the numerical guidance is to regard the guidance objective (e.g. a designed function of the terminal states) as a nonlinear function of the guidance command by onboard models of the entry dynamics and Martian atmosphere, and then generate the guidance command onboard based on predicting and correcting the errors through onboard model integration and nonlinear root searching. The motivation of numerical predictive guidance is the requirement of the future Mars landing exploration mission to significantly improve the landing accuracy and the robustness to the large errors at the entry interface. Compared with trajectory tracking methods, numerical predictive guidance inherently overcomes the weakness of introducing errors from assumptions and the linearization process.

For Mars atmospheric entry, Kluever pointed out that the potential problems of the numerical predictive guidance mainly were due in the errors of a large onboard model bias [150]. Lu proposed a unified predictive entry guidance method which is applicable to vehicles with varying lifting capabilities [135]. Kozynchenko pointed out that the predictive guidance technique was essentially an eigenvalue problem of the differential equation and analyzed the applicability of the predictive guidance method under possible high discrepancies between the onboard dynamic model and the real environment [151]. By adopting the estimation information, the predictive guidance method can also achieve high precision in the terminal conditions under the existence of model biases in the atmosphere and aerodynamic parameters. To deal with the problem of constraint satisfaction, Zheng et al. proposed a constrained numerical predictor-corrector guidance method by introducing the constraint as a penalty term into the traditional nonlinear searching function [152].

The predictive technique is also applied into the optimal guidance method. Unlike the method of onboard trajectory optimization, the optimal guidance method usually obtains a parameterized profile by Pontryagin's minimum principle, and then searches the parameter onboard to generate the guidance command. It is concluded that in aerocapture, the optimal bank angle guidance has a bang-bang structure [153]. Based on this conclusion, the predictive technique is introduced to determine the switching time of the bang-bang structure.

During the powered descent phase, the lander needs to generate the on-line command according to the current states to transfer itself to the pre-designated target. The gravity-turn guidance, for instance, is a typical on-line guidance law that has been widely used in early Moon and Mars landing missions. Cheng et al firstly established the analytical model of gravity-turn guidance by keeping the direction of the thrust aligned with the current velocity but in the opposite orientation [154]. In this way, the velocity of the lander could be decreased effectively and the attitude would maintain vertical before landing due to the gravity force. The gravity-turn guidance is easy to compute and applicable in real missions. However, it is unable to adjust the practical landing site and correct any position error after parachute descent, resulting in a large deviation from the original landing point. Based on this issue, McInnes investigated a gravity-turn guidance that could adjust both the magnitude and the direction of the thrust to improve landing accuracy [155]. Meanwhile, an adaptive tracking control law was designed [156] and safe landing was ensured even if some of the thrusters failed, which enhanced the robustness of the system.

Similar to the zero-effort-miss (ZEM) distance, Ebrahimi et al proposed the concept of zero-effort-velocity (ZEV) error which referred to the deviation of terminal condition if no further control was applied [157]. The ZEM/ZEV concepts were further employed by Furfaro et al in powered descent guidance design and the goal was to generate a proper command that mitigated the errors [158]. It was later proved by Hawkins et al that the ZEM/ZEV guidance was a generalized form of the optimal feedback guidance, and the guidance law was then enhanced with a collision avoidance capability through the combination with waypoint guidance [159]. To further improve the efficiency, Guo introduced waypoints to the guidance algorithm [160]. The waypoint optimization problem in the presence of state constraints is efficiently solved using a quadratic programming technique. It was demonstrated that the proposed waypoint-based guidance algorithm could achieve near-optimal performance with acceptable robustness, while meeting various practical constraints. Zhou et al further improved the ZEM/ZEV guidance law considering the no-subsurface constraints in the powered descent phase [161]. Furthermore, Zhang et al. combined the ZEM/ZEV concepts with the collision avoidance guidance, and developed a feedback collision avoidance guidance law which improves the safety of the Mars landing mission [162].

Other trajectory-independent guidance methods for powered descent phase include, but not limited to, the modified Apollo lunar module terminal descent algorithm (also known as the polynomial guidance) [163], the constrained gradient-based indirect optimal control algorithm [164], the analytical energy-optimal algorithm [165], and the second-order cone programming [166]. A comprehensive comparison of these four methods considering a dispersed environment was performed by Steinfeld. The guidance performance such as robustness, ease of implementation, and numerical stability was also evaluated [17].

4. Prospective on Autonomous Navigation and Guidance Techniques for Mars Pinpoint Landing

High performance navigation and guidance system in the Mars AEDL phase plays an important role in fulfilling a successful pinpoint landing. Although present navigation and guidance technologies can guarantee a safe landing, the accuracy is still not the primary consideration. In order to meet the accuracy requirement for the future pinpoint landing missions, autonomous navigation and guidance is developing to be more robust and accurate.

The limited navigation information remains a problem during the approach and entry phase. In order to introduce more navigation measurements, navigation sensors must be developed at the same time. Although the navigation capability of transceiver Electra has been investigated, radiometric navigation is still laying on the blueprint. The further development of the capability of Doppler and ranging measurements will dramatically improve the reliability of the navigation scheme. Meanwhile, the further development of the Mars Entry Atmospheric Data System (MEADS) may also give an alternative answer to the accurate navigation problem during communication blackout. More importantly, the efficient exploitation of usable navigation information is vital to improve the navigation performance. Therefore, the navigation information optimization should be addressed in future navigation system designs.

The atmosphere density is a main source of uncertainty and disturbance for navigation and guidance. The atmospheric density model should be developed to describe the changing trend of the density more accurately. Also, the navigation filter algorithm should further consider the disturbance and uncertainties such as atmosphere density and aerodynamic coefficients to improve the stability and robustness. The MMAE and desensitized EKF approaches may yield new ideas for the development of better navigation filter algorithms. The future research may focus on simplifying the computation for onboard application. For the trajectory optimization, the consideration of atmosphere density uncertainty is also important to improve the robustness of the optimal trajectories and release the burden of the guidance and control system. Still, rapid and reliable optimization methods still need to be investigated.

Although the Mars Science Laboratory mission has implemented atmospheric guidance, the reference trajectory tracking algorithm developed from the Apollo missions was used because of the low computation cost. The predictor-corrector guidance, which is more robust and accurate, has not been used in practice yet. The rapid development of convex optimization methods will improve the computation efficiency dramatically, which makes on-line guidance practical in the near future. Moreover, the robustness of the guidance algorithm, which can be improved by considering the uncertainties in the Mars landing scenario, should be further investigated in the future.

5. Conclusions

The autonomous navigation and guidance in the Mars approach, entry, descent, and landing (AEDL) phases is a key technology for the pinpoint landing. Based on the present research and development of navigation and guidance technology, this paper reviewed the latest developments and current status of autonomous navigation and guidance design for Mars landing mission. Above all, the technology challenges of autonomous navigation and guidance for the AEDL phases have been discussed here. Then the latest developments of navigation and guidance methods were summarized. Finally, a comprehensive prospective for the development of autonomous navigation and guidance is carried out, which may give new ideas to the mission design.

Acknowledgements

This work was supported in part by the National Basic Research Program of China (973 Program) 2012CB720000, the National Natural Science Foundation of China 61374216, 61304248, 61304226, 61603039, China Postdoctoral Science Foundation 2016M591087, 2017T100041, SAST Foundation SAST2016036, and the Science and Technology Innovation Team of Beijing Institute of Technology.

References

[1] NASA. Solar system exploration: the solar system exploration roadmap for NASA’s Office of Space Science. Jet Propulsion Laboratory, JPL-400-1077, Pasadena, CA, May 2003.

[2] Cui P, Yu Z, Zhu S. Research progress and prospect of autonomous navigation techniques for Mars

entry phase. J Astronautics. 2013; 34(4): 447-456.
DOI: 10.3873/j. issn. 1000-1328. 2013. 04. 001
[3] Braun RD, Manning RM. Mars exploration entry, descent, and landing challenges. J Spacecr Rockets. 2007; 44(2): 310-323.
DOI: 10.2514/1.25116
[4] Mogensen AE. Real-time navigation for Mars final approach using the Mars network (Ph.D. Dissertation), The University of Texas at Austin.
[5] Martin MS, Mendeck GF, Brugarolas PB, et al. In-flight experience of the Mars Science Laboratory Guidance, Navigation, and Control system for Entry, Descent, and Landing. CEAS Space J. 2015; 7(2): 119-142.
DOI: 10.1007/s12567-015-0091-3
[6] Portock BM, Graat EJ, McElrath TM, Watkins MM, and Wawrzyniak GG. Mars exploration rovers cruise orbit determination. In: AIAA/AAS Astrodynamics Specialist Conference, AIAA-2004-4981; 2004.
DOI: 10.2514/6.2004-4981
[7] Crisp JA, Adler M, Matijevic JR, et al. Mars Exploration Rover mission. J Geophys Res Planets. 2003; 108(E12):429-432.
DOI: 10.1029/2002JE002038
[8] Johnson A, Willson R, Cheng Y, et al. Design through operation of an image-based velocity estimation system for Mars landing. Int J Comput Vis. 2007; 74(3):319-341.
DOI: 10.1007/s11263-006-0022-z
[9] Desai PN, Knocke PC. Mars exploration rovers entry, descent, and landing trajectory analysis. J Astronaut Sci. 2007; 55(3):311-323.
DOI: 10.1007/BF03256527
[10] D'Amario LA. Mars exploration rovers navigation results. J Astronaut Sci. 2006; 54(2):129-173.
DOI: 10.1007/BF03256481
[11] Martinmur TJ, Kruizinga GL, Burkhart PD, et al. Mars Science Laboratory interplanetary navigation. J Spacecr Rockets. 2014; 51(4):1014-1028.
DOI: 10.2514/1.A32631
[12] Mendeck GF, Mcgrew LC. Entry guidance design and postflight performance for 2011 Mars Science Laboratory Mission. J Spacecr Rockets. 2014; 51(4):1094-1105.
DOI: 10.2514/1.A32737
[13] Pollard BD, and Chen CW. A radar terminal descent sensor for the Mars Science Laboratory Mission. In: 2009 IEEE Aerospace Conference, Big Sky, MT; 2009.
DOI: 10.1109/AERO.2009.4839463
[14] Braun RD. The Mars Science Laboratory entry, descent, and landing system. J Spacecr Rockets. 2014; 51(4): 993-993.
DOI: 10.2514/1.A33068
[15] Quadrelli MB, Wood LJ, Riedel JE, et al. Guidance, navigation, and control technology assessment for future planetary science missions. J Guid Control Dyn. 2015; 38(7): 1165-1186.
DOI: 10.2514/1.G000525
[16] Karlgaard C, and Schoenenberger M. Mars Science Laboratory entry, descent, and landing trajectory and atmosphere reconstruction. In: AAS/AIAA Spaceflight Mechanics Conference, AAS 2013-0307; 2013.

[17] Steinfeldt BA, Grant MJ, Matz DA, Braun RD, Barton GH. Guidance, navigation, and control system performance trades for Mars pinpoint landing. J Spacecr Rockets. 2010; 47(1): 188-198.
DOI: 10.2514/1.45779
[18] Li S, Jiang X. Review and prospect of guidance and control for Mars atmospheric entry. Prog Aerosp Sci. 2014; 69: 40-57.
DOI: 10.1016/j.paerosci.2014.04.001
[19] D'Souza SN, Sarigul-Klijn N. Survey of planetary entry guidance algorithms. Prog Aerosp Sci. 2014; 68(8): 64-74.
DOI: 10.1016/j.paerosci.2014.01.002
[20] Thornton CL, Border JS. Radiometric tracking techniques for deep-space navigation. Monograph 1, Deep Space Communications and Navigation Series, Jet Propulsion Laboratory, California Institute of Technology, Pasadena, California.
[21] Magenta Books. Delta-differential one way ranging (Delta-DOR) operations. Recommended Practice, CCSDS 506.0-M-1, July, 2010.
[22] Riedel JE, Bhaskaran S, Desai S, et al. Using autonomous navigation for interplanetary missions: the validation of deep space 1 AutoNav. In: Fourth IAA International Conference on Low-Cost Planetary Missions, IAA Paper L-0807; 2000.
[23] Rush B, Bhaskaran S, Synnott SP. Improving Mars approach navigation using optical data. Adv. Astronaut. Sci. 2002; 109(II): 1651-1660.
[24] Ma P, Jiang F, Baoyin H. Autonomous navigation of mars probes by combining optical data of viewing Martian moons and SST data. J Navig. 2015; 68(6): 1-22.
DOI: 10.1017/S0373463315000272
[25] Johnston MD, Graf JE, Zurek RW, et al. The Mars reconnaissance orbiter mission. In: 2003 IEEE Aerospace Conference, Big Sky, MT; 2003.
[26] Bell DJ, Cesarone R, Ely, TA, et al. Mars network: A Mars orbiting communications & navigation satellite constellation. In: 2000 IEEE Aerospace Conference, Big Sky, MT; 2000.
[27] Hastrup RC, Bell DJ, Cesarone RJ, et al. Mars network for enabling low-cost missions. Acta Astronaut. 2003; 52(2): 227-235.
DOI: 10.1016/S0094-5765(02)00161-3
[28] Ely TA, and Guinn JR. Mars approach navigation using Mars network based Doppler tracking. In: AIAA/AAS Astrodynamics Specialist Conference, AIAA 2002-4816; 2002.
DOI: 10.2514/6.2002-4816
[29] Lightsey EG, Mogensen AE. Real-time navigation for Mars missions using the Mars network. J Spacecr Rockets. 2008; 45(3): 519-533.
DOI: 10.2514/1.30974
[30] Downs GS. Interplanetary navigation using pulsating radio sources. NASA Technical Reports N74-34150; 1974.
[31] Chester TJ, and Butman SA. Navigation using X-ray pulsars. NASA Technical Reports N81-27129, 1981.
[32] Sheikh SI, Pines DJ, Wood KS, et al. Spacecraft navigation using X-ray pulsars. J Guid Control Dyn. 2006; 29(1): 49-63.
DOI: 10.2514/1.13331
[33] Sheikh SI. The use of variable celestial X-ray sources for spacecraft navigation. Ph.D. Dissertation, University of Maryland, College Park, Maryland, 2005.

[34] Emadzadeh AA, Speyer JL. Relative navigation between two spacecraft using X-ray pulsars. IEEE Trans Control Syst Technol. 2011; 19(5): 1021-1035.
DOI: 10.1109/TCST.2010.2068049
[35] Graven PH, Collins JT, Sheikh SI, Hanson JE. Spacecraft navigation using X-ray pulsars. In: 7th International ESA Conference on Guidance, Navigation & Control Systems, 2-5 Tralee, County Kerry, Ireland; 2008.
[36] Graven P, Collins J, Sheikh S, et al. XNAV for deep space navigation. In: 31st Annual AAS Guidance and Control Conference, Breckenridge, CO; 2008.
[37] Gendreau KC, Arzoumanian Z, Okajima T. The neutron star interior composition explorer (NICER): an explorer mission of opportunity for soft x-ray timing spectroscopy. In: SPIE Astronomical Telescopes Instrumentation. International Society for Optics and Photonics, 2012: 844313-844313-8.
[38] Winternitz LMB, Hassouneh MA, Mitchell JW, et al. X-ray pulsar navigation algorithms and testbed for SEXTANT. In: 2015 IEEE Aerospace Conference, Big Sky, MT; 2015.
DOI: 10.1109/AERO.2015.7118936
[39] Cui P, Yu Z, Zhu S, et al. Real-time navigation for Mars final approach using X-ray pulsars. In: AIAA Guidance, Navigation, and Control Conference, AIAA 2013-5204; 2013.
DOI: 10.2514/6.2013-5204
[40] Cui P, Wang S, Gao A, et al. X-ray pulsars/doppler integrated navigation for Mars final approach. Adv Space Res. 2016; 57(9): 1889-1900.
DOI: 10.1016/j.asr.2016.02.001
[41] Peter B. de Selding ESA: Mars lander crash caused by 1-second inertial measurement error. http://spacenews.com/esa-mars-lander-crash-caused-by-1-second-inertial-measurement-error/#sthash.PVQ5KoU5.dpuf. November 23, 2016
[42] Ely TA, Bishop RH, Dubois-Matra O. Robust entry navigation using hierarchical filter architectures regulated with gating networks. In: 16th International Symposium on Spaceflight Dynamics Symposium, Pasadena, CA; 2001.
[43] Heyne MC. Spacecraft precision entry navigation using an adaptive sigma point Kalman filter bank. Austin TX: The University of Texas at Austin, 2007.
[44] Dubois-Matra O, Bishop RH. Multi-model navigation with gating networks for Mars entry precision landing. In: AIAA Atmospheric Flight Mechanics Conference, AIAA 2004-5279; 2004.
DOI: 10.2514/6.2004-5279
[45] Zanetti R, Bishop RH. Adaptive entry navigation using inertial measurements. In: 17th Annual Space Flight Mechanics Meeting, Sedona, AZ; 2007.
[46] Kenneth L. An innovative deep space application of GPS technology for formation flying spacecraft. In: AIAA Guidance, Navigation and Control Conference, AIAA 1996-3819; 1996.
DOI: 10.2514/6.1996-3819
[47] Morabito DD. The spacecraft communications black-out problem encountered during passage or entry of planetary atmospheres. Pasadena, California: Jet Propulsion Laboratory, August 2002.
[48] Yu Z, Cui P, Zhu S. Observability-based beacon configuration optimization for Mars entry navigation. J Guid Control Dyn. 2015; 38(4): 643-650.
DOI: 10.2514/1.G000014
[49] Burkhart PD, Ely T, Duncan C, et al. Expected EDL navigation performance with spacecraft to spacecraft radiometric data. In: AIAA Guidance, Navigation, and Control Conference, AIAA 2005-5949; 2005.

DOI: 10.2514/6.2005-5949
[50] Lévesque JF, and de Lafontaine J. Innovative navigation schemes for state and parameter estimation during Mars entry. J Guid Control Dyn. 2007; 30(1): 169-184.
DOI: 10.2514/1.25107
[51] Yu Z, Cui P, Zhu S, et al. Radiometric measurement based navigation and performance trend for Mars landing. In: 67th International Astronautical Congress, Guadalajara, Mexico; 2016.
[52] Edwards CD, Jedrey TC, Schwartzbaum E, Devereaux AS. The Electra proximity link payload for Mars relay telecommunications and navigation. In: 54th International Astronautical Congress, Bremen, Germany; 2003.
[53] Steltzner A, Kipp D, Chen A, et al. Mars Science Laboratory entry, descent, and landing system. In: 2006 IEEE Aerospace Conference, Big Sky, MT; 2006.
DOI: 10.1109/AERO.2006.1655796
[54] Hamkins J, Simon MK, Yuen JH. Autonomous soft-ware-defined radio receivers for deep space applications. Hoboken, New Jersey: Wiley-Interscience, 2006.
[55] Kirk BB, Intrieri PF, Seiff A. Aerodynamic behavior of the Viking entry vehicle: ground test and flight results. J Spacecr Rockets. 1978; 15: 208-212.
DOI:10.2514/3.57307
[56] Gazarik MJ, Wright MJ, Little A, et al. Overview of the MEDLI project. In: 2008 IEEE Aerospace Conference, Big Sky, MT; 2008.
DOI:10.1109/AERO.2008.4526285
[57] Dutta S, Braun RD. Statistical entry, descent, and landing performance reconstruction of the Mars science laboratory. J Spacecr Rockets. 2014; 51: 1048-1061.
DOI:10.2514/1.48239
[58] Chen A, Cianciolo A, Vasavada AR, Karlgaard C, Barnes J, Cantor B, Kass D, Rafkin S, Tyler D. Reconstruction of atmospheric properties from Mars science laboratory entry, descent, and landing. J Spacecr Rockets. 2014; 51: 1062-1075.
DOI:10.2514/1.A32708
[59] Cui P, Ge D, Gao A. Optimal landing site selection based on safety index during planetary descent. Acta Astronaut. 2017; 132: 326-336.
DOI: 10.1016/j.actaastro.2016.10.040
[60] Johnson AE, Ivanov TI. Analysis and testing of a lidar-based approach to terrain relative navigation for precise lunar landing. In: AIAA Guidance, Navigation, and Control Conference, AIAA 2011-6578; 2011.
DOI: 10.2514/6.2011-6578
[61] Guizzo GP, Bertoli A, Torre AD, Magistrati G, Mailland F, et al. Mars and Moon exploration passing through the european precision landing GNC test facility. Acta Astronaut. 2008;63(1-4):74-90. DOI:10.1016/j.actaastro.2007.12.006
[62] Johnson AE, Montgomery JF. Overview of terrain relative navigation approaches for precise lunar landing. In: 2008 IEEE Aerospace Conference. Big Sky, MT; 2008.
DOI: 10.1109/AERO.2008.4526302
[63] Amzajerdian F, Pierrottet D, Petway L, Hines G, Roback V. Lidar systems for precision navigation and safe landing on planetary bodies. In: International symposium on photoelectronic detection and imaging 2011, international society for optics and photonics. Paper 819202-1, Bellingham, WA; 2011.
DOI: 10.1117/12.904062

[64] Busnardo DM, Aitken ML, Tolson R, Pierrottet HD, Amzajerdian F. LIDAR-aided inertial navigation with extended kalman filtering for pinpoint landing over rough terrain. In: 49th AIAA aerospace sciences meeting including the new horizons forum and aerospace exposition. AIAA Paper 2011-428, Orlando, FL; 2011.
DOI: 10.2514/6.2011-428
[65] Amzajerdian F, Petway L, Hines G, Barnes B, Pierrottet D, Lockard G. Doppler Lidar sensor for precision landing on the Moon and Mars. In: 2012 IEEE Aerospace Conference. Big Sky, MT; 2012.
DOI: 10.1109/AERO.2012.6187004
[66] Li S, Peng Y, Lu Y, Zhang L, Liu Y. MCAV/IMU integrated navigation for the powered descent phase of Mars EDL. Adv Space Res. 2010; 46(5): 557-570.
DOI: 10.1016/j.asr.2010.04.028
[67] Zanetti R. Advanced navigation algorithms for precision landing. PhD. Dissertation. Department of Aerospace Engineering and Engineering Mechanics, The University of Texas at Austin, Austin, Texas; 2007.
[68] Ely TA, Heyne M, Riedel JE. Altair navigation performance during translunar cruise, lunar orbit, descent, and landing. J Spacecr Rockets. 2012; 49(2):295-317.
DOI: 10.2514/1.52233
[69] Trawny N, Mourikis AI, Roumeliotis SI. Vision-aided inertial navigation for pin-point landing using observations of mapped landmarks. J Field Robot. 2007; 24(5):357-378.
DOI: 10.1002/rob.20189
[70] Mourikis AI, Trawny N, Roumeliotis SI, Johnson AE, Ansar A, Matthies L, Vision-aided inertial navigation for spacecraft entry, descent, and landing. IEEE Trans Robot. 2009; 25(2): 264-280.
DOI: 10.1109/TRO.2009.2012342
[71] Li S, Cui P, Cui H. Vision-aided inertial navigation for pinpoint planetary landing. Aerosp Sci Technol. 2007; 11(6): 499-506.
DOI: 10.1016/j.ast.2007.04.006
[72] Yu M, Cui H, Tian Y. A new approach based on crater detection and matching for visual navigation in planetary landing. Adv Space Res. 2014; 53(12): 1810-1821.
DOI: 10.1016/j.asr.2013.04.011
[73] Yu Z, Xu R, Cui P. A multi sensor based integrated navigation for pin-point landing on Mars. In: AIAA Guidance, Navigation, and Control Conference, AIAA 2015-1331; 2015.
DOI:10.2514/6.2015-1331
[74] Qin T, Zhu S, Cui P. An innovative navigation scheme of powered descent phase for Mars pinpoint landing. Adv Space Res. 2014; 54(9): 1888-1900.
DOI: 10.1016/j.asr.2014.07.009
[75] Evensen G. Sequential data assimilation with a nonlinear quasi-geostrophic model using Monte Carlo methods to forecast error statistics. J Geophys Res. 1994; 99(C5): 10143-10162.
DOI: 10.1029/94JC00572
[76] Tippett MK, Anderson JL, Bishop CH, Hamill TM, Whitaker JS. Ensemble square root filters. Mon Weather Rev. 2003; 131: 1485-1490.
[77] Evensen G. Sampling strategies and square root analysis schemes for the EnKF. Ocean Dyn. 2004; 54: 539-560.
DOI: 10.1007/s10236-004-0099-2
[78] Carvalho H, Moral PD, Monin A, Salut G. Optimal nonlinear filtering in GPS/INS integration. IEEE

Trans Aerosp Electron Syst. 1997; 33(3): 835-850.
DOI: 10.1109/7.599254
[79] Yang C, Singh T. Efficient particle filtering for road-constrained target tracking. IEEE Trans Aerosp Electron Syst. 2007; 43(4): 1454-1469.
DOI: 10.1109/ICIF.2005.1591850
[80] Park ES, Park SY, Roh KM, Choi KH. Satellite orbit determination using a batch filter based on the unscented transformation. Aerosp Sci Technol. 2010; 14(16): 387-396.
DOI: 10.1016/j.ast.2010.03.007
[81] Chowdhary G, Jategaonkar R. Aerodynamic parameter estimation from flight data applying extended and unscented Kalman filter. Aerosp Sci Technol. 2010; 14(2): 106-117.
DOI: 10.1016/j.ast.2009.10.003
[82] Ahmadi M, Khayatian A, Karimaghaee P. Attitude estimation by divided difference filter in quaternion space. Acta Astronaut. 2012; 75: 95-107.
DOI:10.1016/j.actaastro.2011.12.022
[83] Fu H, Xiao Q, Wu Y, Lou T. Rank filter method. J Mech Strength. 2014; 4: 521-526. DOI:10.16579/j.issn.1001.9669.2014.04.031
[84] Prabhakar A, Fisher J, Bhattacharya R. Polynomial chaos-based analysis of probabilistic uncertainty in hypersonic flight dynamics. J Guid Control Dyn. 2010; 33(1): 222-234.
DOI: 10.2514/1.41551
[85] Pence B, Fathy H, Stein J. A maximum likelihood approach to recursive polynomial chaos parameter estimation. In: 2010 American Control Conference (ACC2010). Baltimore, MD; 2010.
[86] Li J, Xiu D. A generalized polynomial chaos based ensemble Kalman filter with high accuracy. J Comput Phys. 2009; 228(15): 5454-5469.
DOI:10.1016/j.jcp.2009.04.029
[87] Pajonk O, Rosić BV, Litvinenko A, Matthies HG. A deterministic filter for non-Gaussian Bayesian estimation-applications to dynamical system estimation with noisy measurements. Physica D. 2012; 241(7): 775-788.
DOI:10.1016/j.physd.2012.01.001
[88] Pajonk O, Rosić BV, Matthies HG. Sampling-free linear Bayesian updating of model state and parameters using a square root approach. Comput Geosci. 2013; 55: 70-83.
DOI: 10.1016/j.cageo.2012.05.017
[89] Blanchard ED, Sandu A, Sandu C. A polynomial chaos-based Kalman filter approach for parameter estimation of mechanical systems. J Dyn Syst Meas Control. 2010; 132(6): 061404.
DOI: 10.1115/1.4002481
[90] Yu Z, Cui P, Ni M. A polynomial chaos based square-root Kalman filter for Mars entry navigation. Aerosp Sci Technol. 2016; 51: 192-202.
DOI: 10.1016/j.ast.2016.02.009
[91] Li S, Jiang X, Liu Y. Innovative Mars entry integrated navigation using modified multiple model adaptive estimation. Aerosp Sci Technol. 2014; 39: 403-413.
DOI: 10.1016/j.ast.2014.04.009
[92] Xiao Q, Fu H, Wang Z, Zhang Y. Multiple model adaptive rank estimation for integrated navigation during Mars entry. J Navig. 2017; 70: 291-308.
DOI: 10.1017/S037346331600059X
[93] Li S, Jiang XQ, Liu Y. High-precision Mars entry integrated navigation under large uncertainties. J

Navig. 2013; 67: 327-342.
DOI: 10.1017/S0373463313000738
[94] Lou T, Zhao L. Robust Mars atmospheric entry integrated navigation based on parameter sensitivity. Acta Astronaut. 2016; 119: 60-70.
DOI: 10.1016/j.actaastro.2015.11.006
[95] Wang L, Xia Y. Mars entry navigation with uncertain parameters based on desensitized extended kalman filter. IEEE Trans Ind Inform. 2015; 11: 998-1005.
DOI: 10.1109/TII.2015.2463763
[96] Ely TA. Optimal orbits for sparse constellations of Mars navigation satellites. In: AAS/AIAA Spaceflight Mechanics Meeting 2001. Santa Barbara, CA; 2001.
[97] Pirondini F, Fernández AJ. A new approach to the design of navigation constellations around Mars: The MARCO POLO evolutionary system. In: 57th International Astronautical Congress. Valencia, Spain; 2006.
[98] Maessen DC, Gill E. Relative state estimation and observability for formation flying satellites in the presence of sensor noise. Acta Astronaut. 2013; 82: 129-136.
DOI: 10.1016/j.actaastro.2012.03.030
[99] Pastor R, Bishop RH, Gay RS, Striepe SA. Mars entry navigation from EKF processing of beacon data. In: AIAA/AAS Astrodynamics Specialist Conference, AIAA 2000-4426; 2000.
[100] Yu Z, Zhu S, Cui P. Orbit optimization of Mars orbiters for entry navigation: from an observability point of view. Acta Astronaut. 2015; 111: 136-145.
DOI: 10.1016/j.actaastro.2015.02.019
[101] Yu Z, Cui P, Zhu S. On the observability of Mars entry navigation using radiometric measurements. Adv Space Res. 2014; 54(8): 1513-1524.
DOI: 10.1016/j.asr.2014.06.036
[102] Zhao Z, Yu Z, Cui P. A beacon configuration optimization method based on Fisher information for Mars atmospheric entry. Acta Astronaut. 2017, 133: 467-475.
DOI: 10.1016/j.actaastro.2016.11.018
[103] Benito J, Mease KD. Reachable and controllable sets for planetary entry and landing. J Guid Control Dyn. 2010; 33(3): 641-654.
DOI: 10.2514/1.47577
[104] Eren U, Dueri D, Açıkmeşe B. Constrained reachability and controllability sets for planetary precision landing via convex optimization. J Guid Control Dyn. 2015; 38(11): 2067-2083.
DOI: 10.2514/1.G000882
[105] Long J, Gao A, Cui P. Controllable set analysis for planetary landing under model uncertainties. Adv Space Res. 2015; 56: 281-292.
DOI: 10.1016/j.asr.2015.04.019
[106] Betts JT. Survey of numerical methods for trajectory optimization. J Guid Control Dyn. 1998; 21(2): 193-207.
DOI: 10.2514/2.4231
[107] Vinh NX. Optimal trajectories in atmospheric flight. New York, NY: Elsevier Scientific Publishing Company, 1981.
[108] Istratie V. Optimal entry into atmosphere with minimum heat and constraints. In: AIAA Atmospheric Flight Mechanics Conference, AIAA 2004-5282; 2004.
DOI: 10.2514/6.2004-5282

[109] Fahroo F, Ross IM. Costate estimation by a legendre pseudospectral method. J Guid Control Dyn. 2001: 24(2): 270-277.
DOI: 10.2514/2.4709
[110] Benson DAA. Gauss pseudospectral transcription for optimal control. PhD. Dissertation. Department of aeronautics and astronautics, Massachusetts Institute of Technology, Cambridge, MA; 2005.
[111] Rao AV, Clarke KA. Performance optimization of a maneuvering reentry vehicle using a Legendre pseudospectral method. In: AIAA Atmospheric Flight Mechanics Conference, AIAA 2002-4885; 2002.
DOI: 10.2514/6.2002-4885
[112] Grant MJ, Clarky IG, Braun, RD. Rapid entry corridor trajectory optimization for conceptual design. In: AIAA Guidance, Navigation, and Control Conference, AIAA 2010-7810; 2010.
DOI: 10.2514/6.2010-7810
[113] Fahroo F, Ross IM. Direct trajectory optimization by a Chebyshev pseudospectral method. J Guid Control Dyn. 2002; 25(1): 160-166.
DOI: 10.2514/2.4862
[114] Patterson MA, Rao AV. GPOPS-II: A MATLAB software for solving multiple-phase optimal control problems using hp-adaptive Gaussian quadrature collocation methods and sparse nonlinear programming, ACM Transactions on Mathematical Software, 2014; 41(1): 1-37.
DOI: 10.1145/2558904
[115] Jacob GL, Neeler G, Ramanan RV. Mars entry mission bank profile optimization. J Guid Control Dyn. 2014; 37(4): 1305-1316.
DOI: 10.2514/1.G000089
[116] Lavagna M, Parigini C, Armellin R. PSO algorithm for planetary atmosphere entry vehicles multidisciplinary guidance design. In: AIAA/AAS Astrodynamics Specialist Conference, AIAA 2006-6027; 2006.
DOI: 10.2514/6.2006-6027
[117] Grant M, Mendeck G, Mars science laboratory entry optimization using particle swarm methodology. In: AIAA Atmospheric Flight Mechanics Conference, AIAA 2007-6393; 2007.
DOI: 10.2514/6.2007-6393
[118] Arora RK. Reentry trajectory optimization: evolutionary approach. In: the 9th AIAA/ISSMO Symposium on Multidisciplinary Analysis and Optimization, 2002.
DOI: 10.2514/6.2002-5466
[119] Chen G, Wan Z, Xu M, Chen S. Genetic algorithm optimization of RLV reentry trajectory. In: AIAA/CIRA 13th International Space Planes and Hypersonics Systems and Technologies, 2005. DOI: 10.2514/6.2005-3269
[120] Yokoyama N, Suzuki S. Modified genetic algorithm for constrained trajectory optimization. J Guid Control Dyn. 2005; 28(1): 139-144.
DOI: 10.2514/1.3042
[121] Lafleur JL, Cerimele C. Mars entry bank profile design for terminal state optimization. J Guid Control Dyn. 2011; 48 (6): 1012-1024.
DOI: 10.2514/1.51944
[122] Yu Z, Cui P, Gao A. A Novel Trajectory Optimization Method for Mars Atmospheric Entry. In: 66rd International Astronautical Congress. Jerusalem, Israel, 2015.
[123] Acikmese B, Ploen SR. Powered descent guidance algorithm for Mars pinpoint landing. In: AIAA

Guidance, Navigation, and Control Conference, AIAA 2005-6288; 2005.
DOI: 10.2514/6.2005-6288
[124] Dueri D, Açıkmeş B, Scharf P. Customized real-time interior-point methods for onboard powered-descent guidance. J Guid Control Dyn. 2017; 40(2): 197-212.
DOI: 10.2514/1.G001480
[125] Lafleur JL. Trading robustness requirements in Mars entry trajectory design. In: AIAA Atmospheric Flight Mechanics Conference, AIAA 2009-5612; 2009.
DOI: 10.2514/6.2009-5612
[126] Li S, Peng Y, Mars entry trajectory optimization using DOC and DCNLP. Adv Space Res. 2011; 47(3): 440-452.
DOI:10.1016/j.asr.2010.09.005
[127] Yu Z, Zhao Z, Cui P. An observability-based trajectory optimization considering disturbance for atmospheric entry. In: AIAA Guidance, Navigation, and Control Conference, AIAA 2016-1373; 2016.
DOI: 10.2514/6.2016-1373
[128] Tu KY, Munir MS, Mease KD. Bayard DS. Drag-based predictive tracking guidance for Mars precision landing. J Guid Control Dyn. 2000; 23(4): 620-628.
DOI: 10.2514/2.4607
[129] Leavitt JA, Mease KD. Feasible trajectory generation for atmospheric entry guidance. J Guid Control Dyn. 2007; 30(2): 473-481.
DOI: 10.2514/1.23034
[130] Benito JM. Advances in spacecraft atmospheric entry guidance, University of California, Irvine, 2010.
[131] Soler L, Khatib A, Mease K. Entry trajectory planning for higher elevation landing. Adv Aerosp Sci. 2008; 148: 397-412.
[132] Duan G, Navarro MR, Mease KD. Trajectory tracking and online replanning for Mars entry. In: AIAA/AAS Astrodynamics Specialist Conference, AIAA 2016-5444; 2016.
DOI: 10.2514/6.2016-5444
[133] Seebinder D, Buskens C. Real-time atmospheric entry trajectory computation using parametric sensitivities. In: 6th International Conference on Astrodynamics Tools and Techniques; 2016.
[134] Zheng Y, Cui H. Mars atmospheric entry guidance using a sensitivity method. IEEE Trans Aerosp Electron Syst. 2017.
DOI: 10.1109/TAES.2017.2669618
[135] Lu P. Entry guidance: a unified method. J Guid Control Dyn. 2014; 37(3): 713-728.
DOI: 10.2514/1.62605
[136] Brunner CW, Lu P. Comparison of fully numerical predictor-corrector and Apollo skip entry guidance algorithms. In: AIAA Guidance, Navigation, and Control Conference, AIAA 2010-8307; 2010.
DOI: 10.2514/6.2010-8307
[137] Carman G, Ives D, Geller D. Apollo-derived Mars precision lander guidance. In: AIAA Atmospheric Flight Mechanics Conference, AIAA 1998-4570; 1998.
DOI: 10.2514/6.1998-4570
[138] Mendeck G, Carman G. Guidance design for Mars smart landers using the entry terminal point controller. In: AIAA Atmospheric Flight Mechanics Conference, AIAA 2002-4502; 2002.
DOI: 10.2514/6.2002-4502
[139] Harpold JC, Gavert DE. Space shuttle entry guidance performance results. J Guid Control Dyn.

1983; 6(6): 442-447.
DOI: 10.2514/3.8523
[140] Bharadwaj S, Rao A, Mease KD. Entry trajectory tracking law via feedback linearization. J Guid Control Dyn. 1998; 21(5): 726-732.
DOI: 10.2514/2.4318
[141] Saraf A, Leavitt J, Chen D, Mease KD. Design and evaluation of an acceleration guidance algorithm for entry. J Spacecr Rockets. 2004; 41(6): 986-996.
DOI: 10.2514/1.11015
[142] Lu P. Regulation about time-varying trajectories: precision entry guidance illustrated. J Guid Control Dyn. 1999; 22(6): 784-790.
DOI: 10.2514/2.4479
[143] Cho N, Kim Y. Three-dimensional nonlinear differential geometric path-following guidance law. J Guid Control Dyn. 2015; 38(12): 2366-2385.
DOI: 10.2514/1.G001060
[144] Furfaro R, Wibben DR. Mars atmospheric entry guidance via multiple sliding surface guidance for reference trajectory tracking. In: AIAA/AAS Astrodynamics Specialist Conference, AIAA 2012-4435; 2012.
DOI: 10.2514/6.2012-4435
[145] Dai J, Xia Y. Mars atmospheric entry guidance for reference trajectory tracking. Aerosp Sci Technol. 2015; 45: 335-345.
DOI: 10.1016/j.ast.2015.06.006
[146] Yu Z, Cui P, Gao A, Dai J. A robust path-tracking guidance considering uncertainty for Mars atmospheric entry. In: 68th International Astronautical Congress; 2017.
[147] Li S, Jiang X. RBF neural network based second-order sliding mode guidance for Mars entry under uncertainties. Aerosp Sci Technol. 2015, 43: 226-235.
DOI: 10.1016/j.ast.2015.03.006
[148] Talole SE, Benito J, Mease KD. Sliding mode observer for drag tracking in entry guidance. In: AIAA Guidance, Navigation and Control Conference, AIAA 2007-6851; 2007.
DOI: 10.2514/6.2007-6851
[149] Xia Y, Chen R, Pu F, Dai L. Active disturbance rejection control for drag tracking in Mars entry guidance. Adv Space Res. 2014; 38(5): 853-861.
DOI: 10.1016/j.asr.2013.12.008
[150] Kluever C. Entry guidance performance for Mars precision landing. J Guid Control Dyn. 2008; 31(6): 1537-1544.
DOI: 10.2514/1.36950
[151] Kozynchenko AI. Analysis of predictive entry guidance for a Mars lander under high model uncertainties. Acta Astronaut. 2011; 68(1-2): 121-132.
DOI: 10.1016/j.actaastro.2010.08.005
[152] Zheng Y, Cui H, Ai Y. Constrained numerical predictor-corrector guidance for Mars precision landing. J Guid Control Dyn. 2017; 40(1): 179-187.
DOI: 10.2514/1.G000563
[153] Lu P, Cerimele CJ, Tigges MA, Matz DA. Optimal aerocapture guidance. J Guid Control Dyn. 2015; 38(4): 553-565.
DOI: 10.2514/1.G000713

[154] Cheng RK. Lunar terminal guidance. Lunar missions and exploration, edited by C. T. Leondes and R. W. Vance, Wiley, New York, 1964.
[155] McInnes CR. Gravity turn descent with quadratic air drag. J Guid Control Dyn. 1997; 20(2): 393-394.
DOI: 10.2514/2.4052
[156] McInnes CR. Direct adaptive control for gravity-turn descent. J Guid Control Dyn. 1999; 22(2): 373-375.
DOI: 10.2514/2.4392
[157] Ebrahimi B, Bahrami M, Roshanian J. Optimal sliding-mode guidance with terminal velocity constraint for fixed-interval propulsive maneuvers. Acta Astronaut. 2008; 62(10-11): 556-562.
DOI: 10.1016/j.actaastro.2008.02.002
[158] Furfaro R, Selnick S, Cupples M, Cribb M. Non-linear sliding guidance algorithms for precision lunar landing. Adv Astronaut Sci. 2011; 140: 945-964.
[159] Guo Y, Hawkins M, Wie B. Applications of generalized zero-effort-miss/zero-effort-velocity feedback guidance algorithm. J Guid Control Dyn. 2013; 36(3):810-820.
DOI: 10.2514/1.58099
[160] Guo Y, Hawkins M, Wie B. Waypoint-optimized zero-effort-miss/zero-effort-velocity feedback guidance for Mars landing. J Guid Control Dyn. 2013; 36(3):799-809.
DOI: 10.2514/1.58098
[161] Zhou L, Xia Y. Improved ZEM/ZEV feedback guidance for Mars powered descent phase. Adv Space Res. 2014, 54(11): 2446-2455. DOI: 10.1016/j.asr.2014.08.011
[162] Zhang Y, Guo Y, Ma G. Collision avoidance ZEM/ZEV optimal feedback guidance for powered descent phase of landing on Mars. Adv Space Res. 2017; 59(6): 1514-1525.
DOI: 10.1016/j.asr.2016.12.040
[163] Wong EC, Singh G, Masciarelli JP. Autonomous guidance and control design for hazard avoidance and safe landing on Mars. J Spacecr Rockets.
DOI: 10.2514/1.19220
[164] Bryson A, Ho Y. Applied Optimal Control, Hemisphere, New York, 1963.
[165] D'Souza C. An optimal guidance law for planetary landing. In: AIAA Guidance, Navigation, and Control Conference. AIAA 1997-3709; 1997.
DOI: 10.2514/6.1997-3709
[166] Açikmeşe B, Ploen S. Convex programming approach to powered descent guidance for Mars landing. J Guid Control Dyn. 2007; 30(5): 1353-1366.
DOI: 10.2514/1.27553